Energy-Band Structure of Selenium Chains

DORIS J. OLECHNA AND ROBERT S. KNOX*
Research and Engineering Center, Xerox Corporation, Webster, New York
(Received 1 June 1965)

The tight-binding method is applied to the valence and lowest conduction bands of selenium chains. Essentially, the calculations of Reitz have been extended and made quantitative. The general features of his results have been verified, a fact which is of interest because in recent years several variants of his band structure have been proposed. However, in detail, our results are quite different; for example, we find that s-p mixing has a nonnegligible effect. With only slight modification, our computed energy bands for chains are found to be successful in interpreting many details appearing in recent reflectivity data on crystalline selenium.

I. INTRODUCTION

CRYSTALLINE selenium has a lattice consisting of spiral chains oriented along the c axis,[1] each spiral having three atoms per turn with equivalent atoms on adjacent chains forming a hexagonal plane network of atoms. Nearest neighbors lie on the same chain, and second-nearest neighbors lie on adjacent chains. Figure 1 is a diagram of this structure which shows all pertinent distances. A complete description of the selenium structure can be found in Ref. 1. It belongs to either space group D_3^4 (right-handed screw axis) or D_3^6 (left-handed screw axis).[2,3]

Although considerable work has been done on the band structure of selenium,[4–8] it is mostly qualitative or semiquantitative. Von Hippel[4] treated the crystal in a tetragonal approximation (whereas it is, in fact, hexagonal with a screw axis) and Gaspar[5] discussed the electronic states largely in terms of the point group of a selenium atom and its nearest neighbors. The most quantitative and realistic treatment is that of Reitz,[6] who observed that a rather simple tight-binding formalism devolved from the assumption that the bond angles within a selenium chain are 90° (whereas they are, in fact, 105.5° in a crystal). He showed how the departure from 90° could be treated as a perturbation on the 90° case and sketched an approximate band structure for wave vectors parallel to the chain axis (crystal c axis).

The present paper represents primarily an attempt to make Reitz's tight-binding calculation completely quantitative. Hartree-Fock wave functions for Se have recently become available,[9] so that all tight-binding parameters are now calculable; in addition to computing them, we have extended his formalism to include hybridization of the $4p$ bands with s bands. Reitz's set of basis functions included 9 for each wave vector, i.e., three sets of $4p$ orbitals for each of the three atoms in the unit cell. As will be seen in Sec. II, we have increased the basis set to 15 bands by adding $4s$ and $5s$ states on each atom. (It is interesting to note that while the atomic Se configuration lying directly above the ground $4p^4$ configuration is $4p^3 5s$, many authors have assumed otherwise and concerned themselves solely with the much more complex case of $4d$ bands.)

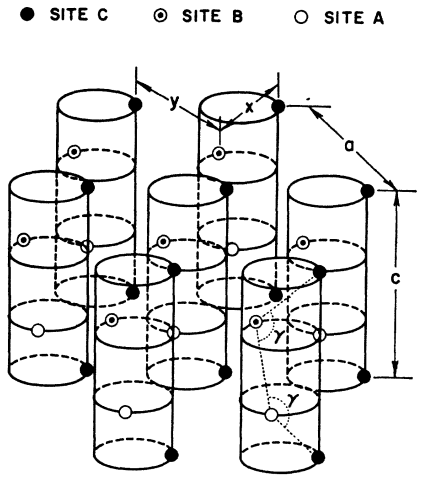

FIG. 1. The crystal structure of selenium. The bonding angle is $\gamma = 105.5°$, $x = 2.32$ Å is the nearest-neighbor distance, $y = 3.46$ Å is the next-nearest-neighbor distance, $a = 4.34$ Å is the distance between like atoms in adjacent chains, and $c = 4.95$ Å is the unit cell dimension along the c axis.

The present calculation is to be regarded as a linear variation calculation, with all the advantages and limitations thereof. It contains "one" adjustable parameter, namely, the choice of exchange potential, which is frequently assumed to be quite arbitrary. Arguments are given which show what a physically reasonable choice of the exchange potential would be. Using it, we were able to closely reproduce the observed band gap. We have restricted the tight-binding sums to members of single chains but discuss the effect this

* Consultant. Permanent address: University of Rochester, Rochester, New York.

[1] M. E. Straumanis, Z. Krist **102**, 432 (1940).
[2] J. Bradley, Phil. Mag. **48**, 477 (1924).
[3] R. H. Asendorf, J. Chem. Phys. **27**, 11 (1957).
[4] A. von Hippel, J. Chem. Phys. **16**, 372 (1948).
[5] R. Gaspar, Acta. Phys. Hung. **7**, 289 (1957).
[6] J. R. Reitz, Phys. Rev. **105**, 1233 (1957). See, E. Behrens, Z. Physik **163**, 140 (1961), for a discussion of the relationship of the Reitz model to a simple cubic Se crystal.
[7] F. Herman, Rev. Mod. Phys. **30**, 102 (1954).
[8] H. Gobrecht and A. Tausend, Z. Physik **161**, 205 (1961).
[9] R. E. Watson and A. J. Freeman, Phys. Rev. **124**, 1117 (1961).

approximation has on comparison with experiments on crystalline Se.

In Sec. II, we outline the general tight-binding method with explicit wave-function overlap and discuss how it applies to the specific case of Se. Section III contains numerical results, and the calculation is compared with experiments in Sec. IV.

II. TIGHT BINDING WITH OVERLAP

In general, the tight-binding method consists of constructing one-electron Bloch wave functions that are linear combinations of different atomic orbitals, computing with them a Hamiltonian matrix, and determining its eigenvalues. Thus, the method is a linear-variation technique, and as many atomic orbitals as practical should be included in the basis set. In the specific case of Se, the effect of considering three nonequivalent atomic sites and the interaction between $4s$, $4p$, and $5s$ states means that approximate energy eigenvalues are determined as solutions of a complex equation of the form

$$\det(H_{ij}-ES_{ij})=0, \tag{1}$$

where H_{ij} is the 15×15 Hamiltonian matrix, and S_{ij} is a 15×15 overlap matrix whose elements are not necessarily equal to zero when $i\neq j$. It can be shown readily that Eq. (1) is expressible in the form of a conventional 30×30 eigenvalue problem,

$$\begin{bmatrix}\begin{pmatrix}B & -C\\ C & B\end{pmatrix}\begin{pmatrix}P & -Q\\ Q & P\end{pmatrix}^{-1}\end{bmatrix}\begin{bmatrix}X_R\\ X_I\end{bmatrix}=E\begin{bmatrix}X_R\\ X_I\end{bmatrix}, \tag{2}$$

where $H_{ij}=B_{ij}+iC_{ij}$, $S_{ij}=P_{ij}+iQ_{ij}$, and X_R and X_I are the real and imaginary parts, respectively, of the eigenvectors associated with Eq. (1).

Throughout this calculation, the Hamiltonian is taken to be

$$H=\mathbf{p}^2/2m+\textstyle\sum_d V_a(\mathbf{r}-\mathbf{R}_d), \tag{3}$$

where $V_a(\mathbf{r}-\mathbf{R}_d)$ is an effective potential due to a single atom located at the lattice point $\mathbf{R}_d$. This potential is assumed to be spherically symmetric and to consist of the sum of the Coulomb potential and an exchange potential. In a selenium atom, the atomic Coulomb potential falls off rapidly enough, as a function of radial distance, that there is negligible overlap with neighboring potentials. Hence, it is a good approximation to consider the crystal Coulomb potential as a sum of atomic potentials. The choice of an exchange potential is not as simple.[10] Since the Slater potential[11] is properly taken as proportional to the cube root of the sum of the charge densities, $[\sum_d\rho(\mathbf{r}-\mathbf{R}_d)]^{1/3}$, it is an overestimate of the crystal exchange potential to use a sum of the cube roots of the individual charge densities, $\sum_d[\rho(\mathbf{r}-\mathbf{R}_d)]^{1/3}$, as we would like to do in order to use the formalism of standard tight-binding theory. In order to approximate the actual exchange potential as a sum of atomic contributions, we estimated how this function should be reduced. One estimate was determined by considering the contributions of the charge densities arising from four neighboring atoms to several points in space and calculating the ratio $[\sum_d\rho(\mathbf{r}-\mathbf{R}_d)]^{1/3}/\sum_d[\rho(\mathbf{r}-\mathbf{R}_d)]^{1/3}$. At all points considered, reduction by a constant factor of 2 produced agreement to within a few percent. This held true throughout the entire range where the exchange potential made a substantial contribution to the total potential. Even this adjustment appeared to be inappropriate, since a band gap of <1 eV resulted (compared with the observed ~2 eV). We therefore tried reducing the exchange even further. In a sense, the Slater exchange potential corresponds to a dielectric constant of 1 and tends to be less accurate for materials with a large dielectric constant, of which Se is one, because of screening effects. A screened exchange potential, introduced by Robinson, Bassani, Knox, and Schrieffer (R.B.K.S.),[12] may be obtained by multiplying the Slater exchange potential by a screening function. As discussed below, our final potential actually corresponds most closely to using $\frac{1}{2}$ of the screened exchange potential.

Following Reitz's method, the matrix elements for the actual 105.5°-bonded Se crystal are obtained by first calculating the elements for a hypothetical 90°-bonded crystal and then treating the effect of 105.5° bonding as perturbation. Figure 2 is a diagram of this hypothetical 90°-bonded structure. The three nonequivalent atomic sites are labeled A, B, and C, and the vectors connecting them are denoted as $\mathbf{R}_\lambda$, $\mathbf{R}_\mu$, and $\mathbf{R}_\nu$. The p functions can be so oriented that they will lie along the orthogonal λ, μ, ν axes. Then, many of the matrix elements will be zero due to the symmetry. The 105.5°-bonded structure is obtained by pulling the hypothetical crystal out along the c axis. The λ, μ, ν axes can remain fixed in space as the crystal is dis-

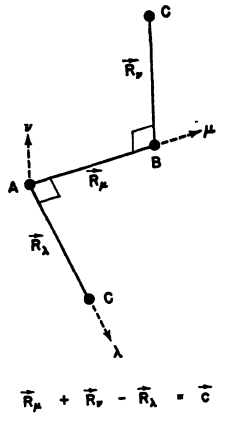

FIG. 2. The selenium chain geometry assuming 90° bonding angles.

[10] See, e.g., W. B. Fowler, thesis, University of Rochester, 1963 (unpublished), pp. 25–30; Phys. Rev. **132**, 1591 (1963).

[11] J. C. Slater, Phys. Rev. **81**, 385 (1951).

[12] J. E. Robinson, F. Bassani, R. S. Knox, and J. R. Schrieffer, Phys. Rev. Letters **9**, 215 (1962).

TABLE I. Representative matrix elements $H_{ij}-ES_{ij}$ [see Eq. (1)]. The symbols are defined in Sec. II and Table II. In the last six matrix elements, the upper sign is used at $\mathbf{k}=0$ and the lower sign at $\mathbf{k}=(0,0,\pi/c)$.

i	j	Matrix element
λA	λA	$N_{\pi\sigma}=V_\pi+V_\sigma+(\epsilon_{4p}-E)$
λA	λB	$e^{i\mathbf{k}\cdot\mathbf{R}_\mu}M_\pi=e^{i\mathbf{k}\cdot\mathbf{R}_\mu}[W_\pi+(\epsilon_{4p}-E)S_\pi]$
λA	λC	$e^{i\mathbf{k}\cdot\mathbf{R}_\lambda}M_\sigma=e^{i\mathbf{k}\cdot\mathbf{R}_\lambda}[W_\sigma+(\epsilon_{4p}-E)S_\sigma]$
λB	λB	$N_\pi=2V_\pi+(\epsilon_{4p}-E)$
λA	μB	$e^{i\mathbf{k}\cdot\mathbf{R}_\mu}[-w(M_\sigma+M_\pi)]$
λA	σA	$V_{s\sigma}$
λA	σB	$e^{i\mathbf{k}\cdot\mathbf{R}_\mu}[wM_{s\sigma}]=e^{i\mathbf{k}\cdot\mathbf{R}_\mu}[w(W_{s\sigma}+(\epsilon_{4p}-E)S_{s\sigma}]$
λA	σC	$e^{i\mathbf{k}\cdot\mathbf{R}_\lambda}M_{\sigma s}=e^{i\mathbf{k}\cdot\mathbf{R}_\lambda}[W_{\sigma s}+(\epsilon_{4s}-E)S_{\sigma s}]$
σA	σA	$N_s=2V_s+(\epsilon_{4s}-E)$
σA	σB	$e^{i\mathbf{k}\cdot\mathbf{R}_\mu}M_s=e^{i\mathbf{k}\cdot\mathbf{R}_\mu}[W_s+(\epsilon_{4s}-E)S_s]$
λA	$\sigma' A$	$V_{s\sigma'}$
λA	$\sigma' B$	$e^{i\mathbf{k}\cdot\mathbf{R}_\mu}[wM_{s\sigma'}\pm(-0.70)M_{s\sigma 2'}]$
λA	$\sigma' C$	$e^{i\mathbf{k}\cdot\mathbf{R}_\lambda}[-M_{s\sigma'}\pm(0.70)M_{s\sigma 2'}]$
σA	$\sigma' A$	$2V_{ss}\pm 2(\epsilon_{4s}-E)S_{ss3}$
σA	$\sigma' B$	$e^{i\mathbf{k}\cdot\mathbf{R}_\mu}[(W_{ss}\pm W_{ss2})+(\epsilon_{4s}-E)(S_{ss}\pm S_{ss2})]$
$\sigma' A$	$\sigma' A$	$2V_s'+(\epsilon_{5s}-E)(1\pm 2S_{ss'})$
$\sigma' A$	$\sigma' B$	$e^{i\mathbf{k}\cdot\mathbf{R}_\mu}[(W_s'\pm W_{s2'})+(\epsilon_{5s}-E)(S_s'\pm S_{s2'})]$

torted. Then $\mathbf{R}_\lambda$, $\mathbf{R}_\mu$, and $\mathbf{R}_\nu$ are still vectors between nearest neighbors, but they no longer lie along the λ, μ, ν directions. Reitz gives the direction cosines of $\mathbf{R}_\lambda$, $\mathbf{R}_\mu$, $\mathbf{R}_\nu$ in relation to the orthogonal λ, μ, ν axes to first order in w,

$$\begin{pmatrix} R_\lambda \\ R_\mu \\ R_\nu \end{pmatrix} \simeq \begin{pmatrix} 1 & -w & -w \\ -w & 1 & w \\ -w & w & 1 \end{pmatrix} \begin{pmatrix} \lambda \\ \mu \\ \nu \end{pmatrix}. \tag{4}$$

For the case of 105.5° bonding, $w=0.144$. In obtaining the matrix elements, only interactions between atoms along a chain and only two-center integrals are considered. *Thus, our calculation is primarily applicable to single Se chains.*

Representative matrix elements for Eq. (1) obtained using the preceding assumptions are given in Table I. In this table, the indices i and j are double indices which refer to both the type and/or direction of the wave function and the atomic site on which it is situated. For example, $i=\lambda A$ means a $4p$ function pointing in the λ direction situated on the A atom, and $i=\sigma B$ means $4s$ situated on the B atom. The primes mean that a $5s$ wave function, rather than $4s$, is involved. As usual, $\mathbf{k}$ is the wave vector. The atomic energy levels are denoted as ϵ_{4s}, ϵ_{4p}, and ϵ_{5s}. The V's, W's, and S's are all two-center integrals defined in Table II. The additional subscript 2 or 3 which appears on some of the symbols means that the expression is evaluated for the second- and third-nearest neighbors along a chain. The quantities $M_{\sigma s}$ and $M_{s\sigma}$, which should be exactly equal to each other's negative, are computed separately and their magnitudes averaged. Note that the matrix elements in Table I are all for the case of 105.5° bonding. When $w=0$ these elements correspond to the case of 90° bonding.

In practice, the two-center integrals appearing in Table II are obtained by first expanding either the wave function or the potential function on one site in spherical harmonics about the other site and then integrating the resulting functions numerically.[13,14] The coefficients of this expansion are the "alpha functions," $\alpha_l(NLM|R,r)$, first introduced by Löwdin[13] and are abbreviated in Table II as $\alpha_{lLM}(F)$; when $F=4s$ or $4p$, it means the corresponding wave function is expanded and, when $F=Z=rV(r)$, a potential function is expanded; R is the distance between the atomic sites; r is the radial distance; $V(r)$ is the potential function; N, L, and M are the quantum numbers of the function which is expanded about another center at which quantum numbers are taken to be n, l, and m. The numbers in this table correspond to a choice of parameters corresponding to roughly $\frac{1}{2}$ the screened exchange potential.

With the exception of the $5s$ wave function, Freeman and Watson's Hartree-Fock wave functions[9] are used throughout these calculations. The functions $P_{nl}(r)$ are defined as r times the radial part of the total one-electron function

$$\psi_{nlm}(r)=(P_{nl}(r)/r)Y_l^m(\theta,\varphi), \tag{5}$$

where $Y_l^m(\theta,\varphi)$ is a spherical harmonic. As will be discussed in the next section, the $5s$ function was added for its variational effect on the lower-lying energy bands, and the actual bands resulting primarily from it are not to be taken too seriously. As a purely variational device, it need not be determined as accurately as the other wave functions. Our $5s$ radial wave function was constructed by requiring it to have four nodes, be normalized, and be orthogonal to the $4s$ state. Its atomic energy level was estimated crudely from the center of gravity of the $4p^35s$ configuration,[15] but the calculation was not sensitive to the choice of ϵ_{5s} within reasonable limits.

In actual practice, we have developed one-parameter formulas for adjusting the exchange potential without recalculating the two-center integrals. To obtain these, the two-center integrals were calculated for two different choices of exchange potential, one half of "Slater exchange" and R.B.K.S. screened exchange, at different distances between atomic sites. From these calculations the following interpolation formulas resulted:

$$\begin{aligned} &W_s=\alpha\bar{W}_s, && W_\sigma=\alpha(0.78+0.22\alpha)\bar{W}_\sigma, \\ &W_\pi=\alpha(0.45+0.55\alpha)\bar{W}_\pi, && W_{s\sigma}=\alpha(1.22-0.22\alpha)\bar{W}_{s\sigma}, \\ &W_{\sigma s}=\alpha(0.45+0.55\alpha)\bar{W}_{\sigma s}, && V_s=\beta\bar{V}_s, \\ &V_\sigma=\beta(1.97-0.97\beta)\bar{V}_\sigma, && V_\pi=\beta(0.52+0.48\beta)\bar{V}_\pi, \\ &V_{s\sigma}=\beta(1.97-0.97\beta)\bar{V}_{s\sigma}, \end{aligned} \tag{6}$$

[13] P. O. Löwdin, Advan. Phys. 5, 1 (1956).
[14] W. Beall Fowler, R. S. Knox, P. J. Eberlein, University of Rochester Report (unpublished); T. H. Keil, University of Rochester Report (unpublished).
[15] C. E. Moore, Natl. Bur. Std. (U. S.) Circ. 467 (1952), Vol. II.

TABLE II. Two-center integrals used in computing matrix elements. All symbols are defined in Sec. II; the numerical values are those used in case (g) of Fig. 3.

$$V_s=\int|\psi_{4s0}(\mathbf{r})|^2V(\mathbf{r}-\mathbf{R})\,d\tau=\int_0^\infty\alpha_{000}(Z)P_{4s}^2(r)dr=-0.0509,$$

$$V_\sigma=\int|\psi_{4p0}(\mathbf{r})|^2V(\mathbf{r}-\mathbf{R})\,d\tau=\int_0^\infty\alpha_{000}(Z)P_{4p}^2(r)dr+\tfrac{2}{5}\int_0^\infty\alpha_{200}(Z)P_{4p}^2(r)dr=-0.173,$$

$$V_\pi=\int|\psi_{4p1}(\mathbf{r})|^2V(\mathbf{r}-\mathbf{R})\,d\tau=\int_0^\infty\alpha_{000}(Z)P_{4p}^2(r)dr-\tfrac{1}{5}\int_0^\infty\alpha_{200}(Z)P_{4p}^2(r)dr=-0.0248,$$

$$V_{s\sigma}=\int\psi_{4s0}^*(\mathbf{r})\psi_{4p1}(\mathbf{r})V(\mathbf{r}-\mathbf{R})\,d\tau=3^{-1/2}\int_0^\infty\alpha_{100}(Z)P_{4p}(r)P_{4s}(r)dr=-0.0792,$$

$$V_s'=\int|\psi_{5s0}(\mathbf{r})|^2V(\mathbf{r}-\mathbf{R})\,d\tau=\int_0^\infty\alpha_{000}(Z)P_{5s}^2(r)dr=-0.141,$$

$$V_{s\sigma}'=\int\psi_{5s0}^*(\mathbf{r})\psi_{4p1}(\mathbf{r})V(\mathbf{r}-\mathbf{R})\,d\tau=3^{-1/2}\int_0^\infty\alpha_{100}(Z)P_{5s}(r)P_{4p}(r)dr=0.108,$$

$$V_{ss}=\int\psi_{5s0}^*(\mathbf{r})\psi_{4s0}(\mathbf{r})V(\mathbf{r}-\mathbf{R})\,d\tau=\int_0^\infty\alpha_{000}(Z)P_{5s}(r)P_{4s}(r)dr=0.03,$$

$$W_s=\int\psi_{4s0}^*(\mathbf{r})V(\mathbf{r})\psi_{4s0}(\mathbf{r}-\mathbf{R})\,d\tau=\int_0^\infty\alpha_{000}(4s)P_{4s}(r)Zdr=-0.108,$$

$$W_\sigma=\int\psi_{4p0}^*(\mathbf{r})V(\mathbf{r})\psi_{4p0}(\mathbf{r}-\mathbf{R})\,d\tau=\int_0^\infty\alpha_{100}(4p)P_{4p}(r)Zdr=0.189,$$

$$W_\pi=\int\psi_{4p1}^*(\mathbf{r})V(\mathbf{r})\psi_{4p1}(\mathbf{r}-\mathbf{R})\,d\tau=\int_0^\infty\alpha_{111}(4p)P_{4p}(r)Zdr=0.0537,$$

$$W_{s\sigma}=\int\psi_{4s0}^*(\mathbf{r})V(\mathbf{r})\psi_{4p0}(\mathbf{r}-\mathbf{R})\,d\tau=3^{1/2}\int_0^\infty\alpha_{010}(4_p)P_{4s}(r)Zdr=0.305,$$

$$W_{s\sigma}=\int\psi_{4p0}^*(\mathbf{r})V(\mathbf{r})\psi_{4s0}(\mathbf{r}-\mathbf{R})\,d\tau=3^{-1/2}\int_0^\infty\alpha_{100}(4s)P_{4p}(r)Zdr=-0.0923,$$

$$W_s'=\int\psi_{5s0}^*(\mathbf{r})V(\mathbf{r})\psi_{5s0}(\mathbf{r}-\mathbf{R})\,d\tau=\int_0^\infty\alpha_{000}(5s)P_{5s}(r)Zdr=0,$$

$$W_{s\sigma}'=\int\psi_{5s0}^*(\mathbf{r})V(\mathbf{r})\psi_{4p0}(\mathbf{r}-\mathbf{R})\,d\tau=3^{1/2}\int_0^\infty\alpha_{010}(4p)P_{5s}(r)Zdr=0.006,$$

$$W_{ss}=\int\psi_{5s0}^*(\mathbf{r})V(\mathbf{r})\psi_{4s0}(\mathbf{r}-\mathbf{R})\,d\tau=\int_0^\infty\alpha_{000}(4s)P_{5s}(r)Zdr=0.002,$$

$$S_s=\int\psi_{4s0}^*(\mathbf{r})\psi_{4s0}(\mathbf{r}-\mathbf{R})\,d\tau=\int_0^\infty\alpha_{000}(4s)P_{4s}(r)rdr=0.163,$$

$$S_\sigma=\int\psi_{4p0}^*(\mathbf{r})\psi_{4p0}(\mathbf{r}-\mathbf{R})\,d\tau=\int_0^\infty\alpha_{110}(4p)P_{4p}(r)rdr=-0.332,$$

$$S_\pi=\int\psi_{4p1}^*(\mathbf{r})\psi_{4p1}(\mathbf{r}-\mathbf{R})\,d\tau=\int_0^\infty\alpha_{111}(4p)P_{4p}(r)rdr=0.174,$$

$$S_{s\sigma}=\int\psi_{4s0}^*(\mathbf{r})\psi_{4p0}(\mathbf{r}-\mathbf{R})\,d\tau=3^{1/2}\int_0^\infty\alpha_{010}(4p)P_{4s}(r)rdr=-0.302,$$

$$S_{\sigma s}=\int\psi_{4p0}^*(\mathbf{r})\psi_{4s0}(\mathbf{r}-\mathbf{R})\,d\tau=3^{-1/2}\int_0^\infty\alpha_{100}(4s)P_{4p}(r)rdr=0.302,$$

$$S_s'=\int\psi_{5s0}^*(\mathbf{r})\psi_{5s0}(\mathbf{r}-\mathbf{R})\,d\tau=\int_0^\infty\alpha_{000}(5s)P_{5s}(r)rdr=0.132,$$

$$S_{s\sigma}'=\int\psi_{5s0}^*(\mathbf{r})\psi_{4p0}(\mathbf{r}-\mathbf{R})\,d\tau=3^{1/2}\int_0^\infty\alpha_{010}(4p)P_{5s}(r)rdr=-0.153,$$

$$S_{ss}=\int\psi_{5s0}^*(\mathbf{r})\psi_{4s0}(\mathbf{r}-\mathbf{R})\,d\tau=\int_0^\infty\alpha_{000}(4s)P_{5s}(r)rdr=-0.28.$$

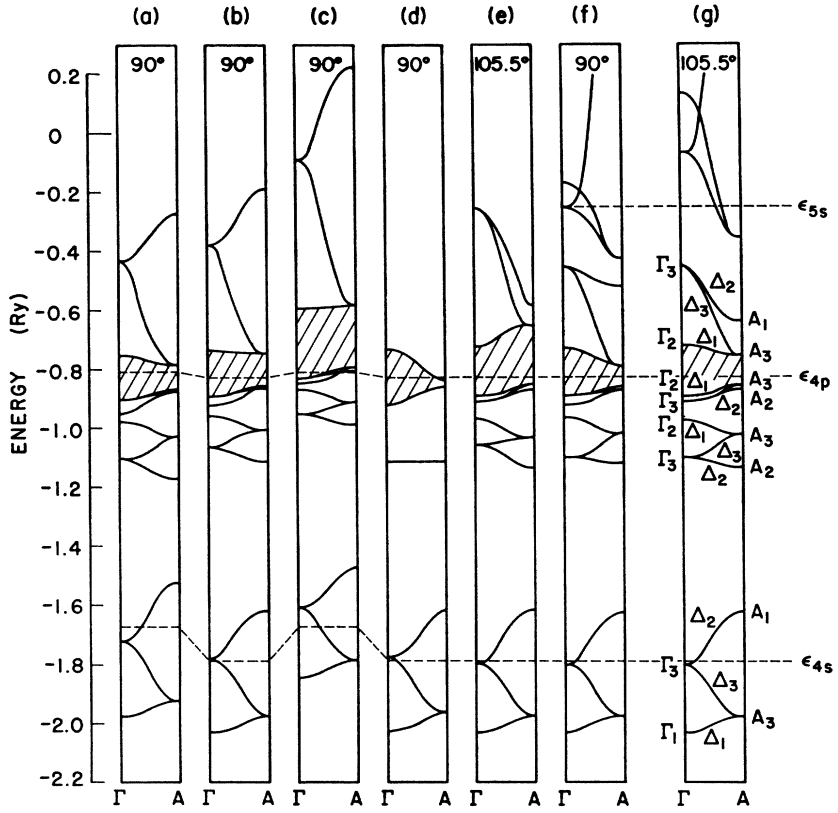

FIG. 3. The results of varying several parameters in the computation of the energy-band structure of selenium chains, such as potential function, hybridization, bonding angle (shown at top), and atomic energy level (dashed lines). The section lines denote the forbidden gap. The exchange potentials used are: screened exchange in case (a); $\frac{1}{2}$ screened exchange in cases (b), (d), (e), (f), and (g); zero exchange in case (c). In case (d), there is no s-p mixing. Case (g) represents our final band structure (see text).

where a bar over a capital letter indicates that the quantity is calculated with one half of the "Slater exchange" potential, $\alpha=0.838t+0.581$ and $\beta=\exp(3.26t-1.63)$, with the exchange potential taken as proportional to $t\Sigma_d[\rho(r-R_d)]^{1/3}$. These equations were further checked by observing that they approached the proper limit for the case of zero exchange. The parameters corresponding to our final results (see below) are $\alpha=0.66$, $\beta=0.27$.

III. NUMERICAL RESULTS

The effects of using "relativistic" atomic energy levels, choice of potential function, hybridization, and bonding angle on the energy-band structure are summarized in Fig. 3. These band structure curves have generally been computed only at the points $k_z=0$ and $k_z=\pi/c$, but certain of the calculations were carried out at intermediate k_z values to verify that they were smoothly varying. The dotted lines are the atomic energy levels. With the exception of cases (a) and (c), they are relativistic atomic energy levels as computed from the tables of Herman *et al.*[16] The major effect of the use of relativistic atomic energy levels is to increase the separation of the 4s- and 4p-like bands without causing much change in their general shape. Cases (a), (b), and (c) are included to show the effect of the choice of exchange potential. They correspond to, respectively, screened exchange, $\frac{1}{2}$ screened exchange, and zero exchange. The effect of decreasing the potential function is to increase the band gap. The remaining curves shown are for the same choice of exchange potential, that of $\frac{1}{2}$ screened exchange. Case (d) shows the effect of neglecting s-p hybridization, namely, the disappearance of splittings and a sharp decrease in the band gap. When the bonding angle was increased to 105.5°, case (e), which is to be compared with case (c), the conduction bands were observed to be strongly dependent upon the choice of potential. To stabilize these bands, a 5s band was added in cases (f) and (g); in any linear variational calculation, it is the lower-lying energy bands that are the most accurately determined. The fact that this device does indeed stabilize the lowest conduction bands can be seen by comparing cases (b) and (e) with cases (f) and (g).

Case (g) represents our final calculated results. A direct band gap at π/c of 1.4 eV is obtained which compares favorably with the experimentally determined gap of about 2 eV.[17] Actually, a gap of 2 eV could have been obtained by further but perhaps unphysical reduction of the amount of exchange potential. By fitting a cosine function to the energy bands, effective masses at the point A were estimated, in units of the free

[16] F. Herman, C. D. Kuglin, K. F. Cuff, and R. L. Kortum, Phys. Rev. Letters **11**, 541 (1963).

[17] V. Prosser, Czech. J. Phys. **10B**, No. 4, 306 (1960).

electron mass, to be: 2.2 for the lowest conduction band, 1.9 for the top valence band, and 1.3 for the next highest valence band. By simply varying the bonding angle, we determined values of the corresponding "deformation potentials" for this chain structure (which might be of interest for electron-phonon interactions in which only longitudinal phonons along a chain are important). These were 4.3 eV for the bottom conduction state (A_3), 0.3 eV for the top valence state (A_3), and -0.6 eV for the next lower lying valence state (A_2).

Since so many authors have concerned themselves with the effect of $4d$ bands, we have tried to see if a $4d$ band would have a significant effect on our calculation. A $4d$ wave function was constructed in a manner similar to that by which we constructed a $5s$ wave function. From the atomic spectrum, we estimated that its atomic energy level would lie 0.05 Ry above ϵ_{5s}. Assuming that the angular dependence of the various $4d$ functions could be suitably accounted for by considering a single spherically symmetric function, we substituted the radial part of the $4d$ function for that of the $5s$ in the above formalism. There was negligible effect on the valence bands and on the lowest lying conduction band. It might be pointed out that adding a complete set of $4d$ bands, along with a $5s$ band (for none of which Hartree-Fock functions are known), would be a rather large task, but might be essential in order to obtain a reliable prediction of band-to-band oscillator strengths (see Sec. IV).

IV. DISCUSSION

The present calculation can be of help in evaluating prior work that relates to the band structure of selenium. We shall briefly comment on some of this work. Gaspar[5] qualitatively investigated the band structure of Se in terms of the point group of an atom and its nearest neighbors, taking into account interactions between atoms on adjacent chains. He stressed the importance of hybridization and assumed, incidentally, that the lowest excited state of Se belonged to the $4p^3 4d$ configuration. Gobrecht and Tausend have written several papers in which they relate their experimental data to their interpretations of the theoretical calculations of Reitz and Gaspar. In their first paper,[8] they modify Gaspar's calculation so that all of the $4p$ bands lie beneath the $4d$ bands and ascribe peaks in the absorption coefficient and index of refraction at about 3 and 21 μ as being due to $p \rightarrow p$ band transitions, with the large peaks at about 2 eV as being due to $p \rightarrow d$ transitions. In more recent work,[18] no mention is made of the 21-μ peaks, but the same interpretation is applied to the other peaks. By applying classical theory to Faraday rotation data, they have also attempted to give values for effective masses[18,19] which are generally much larger than those we calculate. Sobolev[20] makes no specific mention of any transitions occurring in Se at either 3 or 21 μ and explains other transitions by applying one aspect of Gaspar's theory, namely, the possible existence of a very narrow vacant p band lying either "in the band gap" or in the (d-like) conduction band. We choose to ignore the 3-μ band, since it occurs in only certain samples and may be an impurity effect; the 21-μ band is undoubtedly vibrational in origin. Cheglokov[21] analyzes Gobrecht and Tausend's absorption coefficient data by a simple tight-binding method in which he considers only a subset of the p-type bands, i.e., the solution of 6×6 secular equation which does not contain the effects of the uppermost set of p-type bands, and interprets transitions at 3 and 21 μ as being due to free carrier valence-to-valence-band transitions. Hulin[22] has done a calculation for tellurium, using the method of linear combination of atomic orbitals, in which he includes the effects of spin-orbit coupling and atoms on adjacent chains. Double group selection rules are given in his results. He finds that the behavior of the energy bands can be quite complex, with the maxima of the valence bands and minima of the conduction bands existing on, although he does not ascertain exactly where on, the hexagonal plane faces of the Brillouin zone. Robin-Kandare and Robin[23] have measured the absorption coefficient in the region from 4 to 110 eV for thin films of amorphous selenium. They interpret their data using Reitz's model, attributing the absorption edge to transitions between the second and third groups of p bands, a set of peaks at about 5 eV to transitions from the second group of p bands to d bands, and a large maximum at 9 eV to transitions between the first and third groups of p bands. Stuke and Keller[24] have measured the reflectivity for single-crystal hexagonal selenium in the region 1.8 to 4.1 eV for polarization parallel and perpendicular to the chain direction. Their results are in good agreement with the experimental results summarized in Prosser's paper[17] and do not show the crossing of the curves that would be indicated by the measurements of Gobrecht and Tausend.[8,18] To interpret their data they propose a crude band model in which they assume that the energy extrema are at $k=0$ and attribute reflectivity peaks to certain direct transitions.

Since Stuke and Keller's data[24] appear to cover the widest range with the highest resolution, we have chosen it to discuss our band calculations. Most of the features in their reflectivity data can be explained with our energy-band results with only minor adjustments in

[18] H. Gobrecht and A. Tausend, in *Proceedings of the International Conference on Semiconductor Physics, Paris 1964* (Academic Press Inc., New York, 1965).

[19] H. Gobrecht, A. Tausend, and J. Hertel, Z. Physik **178**, 19 (1964).

[20] V. V. Sobolev, Dokl. Akad. Nauk SSSR **151**, 1308 (1963) [English transl.: Soviet Phys.—Dokl. **8**, 815 (1964).

[21] E. I. Cheglokov, Fiz. Tver. Tela **6**, 1845 (1964) [English transl.: Soviet Phys.—Solid State **6**, 1451 (1964)].

[22] M. Hulin, Ann. Phys. (Paris) **8**, 647 (1963).

[23] S. Robin-Kandare and J. Robin, *Proceedings of the International Conference on Semiconductor Physics, 1960* (Academic Press Inc., New York, 1961).

[24] J. Stuke and H. Keller, Phys. Status Solidi **7**, 189 (1964).

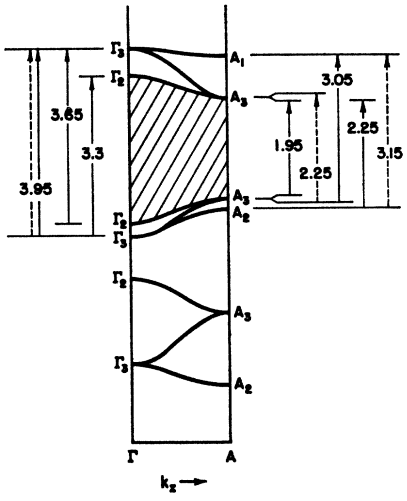

FIG. 4. Direct allowed optical transitions in a proposed selenium-chain band scheme. The dotted and solid arrows correspond, respectively, to light polarized parallel and perpendicular to the c axis; the numbers are energies in electron volts.

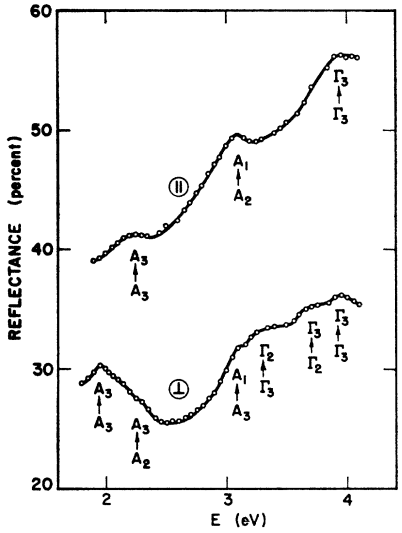

FIG. 5. Room-temperature crystalline-Se reflectivity data of Stuke and Keller (Ref. 24) showing the transitions proposed in Fig. 4.

the conduction bands. The irreducible representations of our energy eigenvectors were determined with the aid of prior group-theoretical treatments of hexagonal selenium.[3,25] Noting that vectors perpendicular to the **c** axis, **x** and **y**, transform as Γ_3, and the vector parallel to the **c** axis, **z**, transforms as Γ_2, we find, by taking the direct products, that the direct allowed optical transitions are[21,22]: $A_1 \rightarrow A_2$, $A_3 \rightarrow A_3$, $\Gamma_1 \rightarrow \Gamma_2$, and $\Gamma_3 \rightarrow \Gamma_3$ for light polarized parallel to **c**; and $A_1 \rightarrow A_3$, $A_2 \rightarrow A_3$, $A_3 \rightarrow A_3$, $\Gamma_1 \rightarrow \Gamma_3$, $\Gamma_2 \rightarrow \Gamma_3$, and $\Gamma_3 \rightarrow \Gamma_3$ for light polarized perpendicular to c. Figure 4 is an energy-band diagram showing the pertinent transitions. The valence bands are exactly those which we obtain in case (g) of Fig. 3. The conduction bands have been adjusted slightly to agree with Stuke and Keller's data; in particular, A_3 and Γ_2 are raised by 0.05 Ry to reproduce a band gap, and Γ_3 is lowered by 0.17 Ry. Note that the degeneracies at A_3 would be removed by the spin-orbit interaction. A value of 0.297 eV for the $4p$-shell spin-orbit energy of Se was earlier deduced by one of us (R.S.K.)[26] from the atomic spectrum; this value is reproduced to within 6% by the use of Watson and Freeman's wave functions. Naturally the splitting in the solid will not be precisely 0.3 eV but will be of this order of magnitude. The dotted and solid arrows refer to, respectively, parallel and perpendicular polarizations. Figure 5 is a redrawing of Stuke and Keller's reflectivity data upon which our proposed optical transitions are indicated. It has been suggested that the first rise in the absorption coefficient might contain an intrinsic exciton peak superimposed upon the absorption edge.[27] In this case, the lowest conduction band shown in Fig. 4 would have to be shifted to still slightly higher energy. At the present stage of refinement of our work, we have not attempted to analyze the effect of excitons on the spectrum but this is clearly an area for future study.

As a check on the wave functions resulting from our calculation, we have evaluated the oscillator strength for the $A_3 \rightarrow A_3$ transition which presumably accounts for the lowest absorption edge. The result is 0.005, strongly disagreeing with the rather large oscillator strength of 15 deducted by Hartke and Regensberger,[27] who note that the experimental number may be an overestimate because of their approximations to the density of valence- and conduction-band states. While this discrepancy is surely the worst one resulting from our calculation, we believe that it can be explained in part by an insufficient admixture of $4d$ and $5s$ functions into our conduction band states. The result of 0.005 is obtained using the single $5s$ (or quasi-$4d$) function admixture, and it will increase sharply with the fraction of even-parity atomic states admixed. This point deserves considerable further study.

In summary, we may say that our results confirm Reitz's proposed band structure, but we would like to stress the important effect that s-p hybridization has on the band structure. Note that even when we considered only 12 bands the distance between the 9th and 10th was of the order of magnitude of the experimentally determined band gap. We would also like to comment on the relevance of our chain model to real crystals. A chain calculation should be expected to explain the gross but not the fine features of either hexagonal or amorphous selenium. In the case of hexagonal selenium, the proximity of atoms on adjacent chains will have a secondary but probably noticeable

[25] A. Nussbaum, Proc. IRE **50**, 1762 (1962).
[26] R. S. Knox, Xerox Research and Engineering Division Laboratories Report No. RL 63-59 (unpublished).
[27] J. L. Hartke and P. J. Regensberger, Phys. Rev. **139**, A970 (1965).

effect on the band structure.[28] For amorphous selenium, deviations from perfect chain structure will be important, but it is conceivable that the bulk of the valence and conduction electrons exist in states resembling those computed here.

Tight-binding theory produces good results for the valence bands, as can be seen by their general invariance across Fig. 3. However, the conduction bands probably need a more sophisticated treatment (such as orthogonalized plane wave or augmented plane wave) which will take into account more efficiently the effect of both the $5s$ and $4d$ bands and that of atoms on adjacent chains. In any event, it is highly unlikely that the uppermost set of $4p$ bands will turn out to be as narrow as has been proposed by some authors.

[28] *Note added in proof.* In this connection, D. B. McKenney has called the authors' attention to the work of W. J. Choyke and L. Patrick [Phys. Rev. **108**, 25 (1957)] and that of F. Eckart and W. Henrion [Phys. Status Solidi **2**, 841 (1962)] in which there appear strong indications that the lowest band gap is indirect in hexagonal Se. Absorption which has the quantitative characteristics of indirect transitions even appears in amorphous Se [D. B. McKenney, M.S. thesis, University of Rochester, 1965 (unpublished)]. We suspect, as does McKenney, that points of the zone other than Γ and A are involved, as in Hulin's model of Te (Ref. 22). We are proceeding to investigate interchain interactions in order to determine the band structure away from the $(0,0,k_z)$ direction.

ACKNOWLEDGMENTS

We would like to express our deepest appreciation to W. B. Fowler and T. H. Keil for the use of their computer programs at various stages of the calculation. Thanks are also due to J. L. Hartke for many stimulating discussions and to P. J. Eberlein and the staff of the University of Rochester Computer Center for their valuable suggestions.

PHYSICAL REVIEW VOLUME 140, NUMBER 3A 1 NOVEMBER 1965

The Electronic Band Structure of Arsenic. II. Self-Consistent Approach*

STUART GOLIN†‡

Department of Physics and Institute for the Study of Metals, University of Chicago, Chicago, Illinois

and

Service de Physique du Solide et de Résonance Magnétique, Centre d'Etudes Nucléaires, Saclay, France

(Received 24 May 1965)

The band structure of arsenic was calculated by the orthogonalized plane-wave method. The Coulomb potential of the valence electrons was calculated self-consistently to within 0.01 hartree. Spin-orbit coupling was put in *a posteriori*; the other relativistic effects as well as correlation and exchange among the valence electrons were not put into the calculation, but the magnitudes of these omissions were estimated. The self-consistent valence potential is found to compare favorably with the potential calculated in the tight-binding limit, and unfavorably with other *ad hoc* valence potentials often assumed in band-structure calculations. The band structure thus calculated is very similar to the band structure previously calculated by the pseudopotential method.

1. INTRODUCTION

THIS paper describes a first-principle orthogonalized plane-wave (OPW) calculation[1,2] for the semimetal arsenic; the crystal potential was computed self-consistently to within 0.01 Hartree. As is well known, the calculation of the crystal potential is the most important part of any band structure calculation. Once the potential is given, the band structure, at least for a simple system, follows in a more or less straightforward manner.

The potential seen by the valence electrons divides neatly into two parts: that due to the ion cores and that due to the valence electrons. The self-energy of a crystal wave function in the Hartree scheme is negligible. The potential due to the ion cores can be accurately calculated in a more or less straightforward manner as seen below. However the calculation of the valence contribution to this potential is considerably more difficult and one often resorts to various *ad hoc* assumptions about the distribution of the valence charge. One popular and successful assumption for metals,[3,4] that the valence charge distribution is uniform, is shown in this paper to be poor for arsenic. The resulting band structure thus depends on these *ad hoc* assumptions which do not allow any direct test of the more

* Work supported in part by the National Science Foundation and the U. S. Office of Naval Research.

† Present address: Department of Mining, Metallurgy, and Petroleum Engineering, University of Illinois, Urbana, Illinois.

‡ National Science Foundation post-doctoral fellow.

[1] C. Herring, Phys. Rev. **57**, 1169 (1940).

[2] For a review of the OPW method, see T. O. Woodruff, in *Solid State Physics*, edited by F. Seitz and D. Turnbull (Academic Press Inc., New York, 1959), Vol. 4, p. 367.

[3] V. Heine, Proc. Roy. Soc. (London) **A240**, 340, 354, 361 (1957).

[4] L. M. Falicov, Phil. Trans. Roy. Soc. London, **A255**, 55 (1962).